

# Beyond the stop: Oxadiazole TRIDs restore LRBA protein expression in nonsense-driven primary immunodeficiency

Ignazio Fiduccia,<sup>1</sup> Emanuele Vitale,<sup>1</sup> Riccardo Varrica,<sup>1</sup> Davide Ricci,<sup>1</sup> Sefora Marino,<sup>1</sup> Antonino Zito,<sup>1</sup> Andrea Pace,<sup>1</sup> Alain Colige,<sup>2</sup> Michel Moutschen,<sup>3,4</sup> Yasmin Borutzki,<sup>5</sup> Andrea Bileck,<sup>5</sup> Samuel M. Meier-Menches,<sup>5</sup> Laura Lentini,<sup>1</sup> and Ivana Pibiri<sup>1</sup>

<sup>1</sup>Department of Biological, Chemical and Pharmaceutical Sciences and Technologies, University of Palermo, Viale delle Scienze Parco d'Orleans II Ed. 17, 90128 Palermo, Italy; <sup>2</sup>Laboratory of Connective Tissues Biology, GIGA Institute, University of Liège, 4000 Liège, Belgium; <sup>3</sup>General Internal Medicine and Clinical Immunology, Centre Hospitalier Universitaire de Liège, 4000 Liège, Belgium; <sup>4</sup>Immunobiology, GIGA Institute, University of Liège, 4000 Liège, Belgium; <sup>5</sup>Department of Analytical Chemistry, University of Vienna, 1090 Vienna, Austria

**Nonsense mutations are among the genetic causes of LRBA (lipopolysaccharide-responsive beige-like anchor) deficiency, a rare autosomal-recessive immunodeficiency disorder. These mutations introduce premature stop codons, leading to the loss of LRBA protein expression. Following the recent market withdrawal of ataluren, the only approved translational readthrough-inducing drug (TRID), there is an urgent need for alternative therapeutic options. In this study, we investigated the efficacy of three 1,2,4-oxadiazole-based TRIDs—NV848, NV914, and NV930—using primary fibroblasts from a patient homozygous for the R1683X nonsense mutation. All compounds restored full-length LRBA protein with correct cytoplasmic localization, as confirmed by western blot and immunofluorescence, outperforming ataluren in readthrough efficiency. NV848 exhibited the strongest activity and uniquely increased LRBA mRNA levels, suggesting transcript stabilization. In contrast, NV930 and NV914 induced readthrough without stabilizing mRNA. Global proteomic profiling revealed minimal off-target effects for NV848, limited protein modulation by NV914, and widespread variations of 828 proteins by NV930, affecting pathways related to vesicular transport and mRNA splicing. However, network analysis revealed poor connectivity among differentially expressed proteins, with LRBA unrelated to any regulated cluster. These findings highlight the reported molecules as promising candidates for precision therapy in LRBA deficiency and shed light on the broader cellular impact of TRIDs.**

## INTRODUCTION

Inborn errors of immunity (IEIs) are a group of monogenic disorders resulting from pathogenic germline variants in single genes. Clinical manifestations of these conditions are severe infections, autoimmunity, autoinflammation, allergies, bone marrow failure, and malignancies. The 2024 update by the International Union of Immunolog-

ical Societies (IUIS) Expert Committee has identified 559 distinct IEIs linked to variants in 508 genes, emphasizing the rapid rate of gene discovery facilitated by advancements in next-generation sequencing technologies.<sup>1</sup>

Among the various single-nucleotide changes that can cause genetic disease, nonsense mutations are particularly detrimental. These mutations account for approximately 11% of all genetic disorders<sup>2,3</sup> and introduce premature termination codons (PTCs) into the coding sequence of genes. Moreover, their presence likely triggers the nonsense-mediated mRNA decay (NMD) pathway, thereby limiting protein synthesis. Consequently, the affected mRNA transcripts are degraded, and those skipping the NMD would produce truncated and un-functional polypeptides.<sup>4,5</sup>

Lipopolysaccharide-responsive and beige-like anchor protein (LRBA) deficiency exemplifies an IEI caused by such nonsense mutations. According to the 2024 IUIS classification (IUIS IEI Classification Table, Category 4), LRBA deficiency falls under “Diseases of immune dysregulation.”<sup>1</sup>

This autosomal-recessive condition results from biallelic loss-of-function variants in the LRBA gene. The 319 kDa LRBA protein belongs to the BEACH-domain family. It is ubiquitously expressed in all tissues and regulates endosomal vesicular trafficking, a process essential for the proper localization and stability of cytotoxic T

Received 12 August 2025; accepted 15 December 2025;  
<https://doi.org/10.1016/j.omtn.2025.102808>.

**Correspondence:** Laura Lentini, Department of Biological, Chemical and Pharmaceutical Sciences and Technologies, University of Palermo, Viale delle Scienze Parco d'Orleans II Ed. 17, 90128 Palermo, Italy.  
**E-mail:** [laura.lentini@unipa.it](mailto:laura.lentini@unipa.it)

**Correspondence:** Ivana Pibiri, Department of Biological, Chemical and Pharmaceutical Sciences and Technologies, University of Palermo, Viale delle Scienze Parco d'Orleans II Ed. 17, 90128 Palermo, Italy.  
**E-mail:** [ivana.pibiri@unipa.it](mailto:ivana.pibiri@unipa.it)



lymphocyte-associated protein 4 (CTLA-4). The absence or dysfunction of LRBA leads to accelerated degradation of CTLA-4, resulting in T cell hyperactivation.<sup>6</sup> However, it is likely that the absence of LRBA affects the membrane expression of other proteins and has an impact on natural immune cells and non-lymphoid tissues.

Clinically, LRBA deficiency presents with a spectrum of symptoms, including hypogammaglobulinemia, lymphoproliferation, chronic diarrhea, and severe autoimmunity. Patients often present recurrent respiratory infections from early childhood, along with autoimmune cytopenias and inflammatory bowel disease, underlining the critical role of LRBA in immune homeostasis.<sup>7–10</sup>

Translational readthrough-inducing drugs (TRIDs) offer a promising precision therapy for IEs caused by PTCs.<sup>11,12</sup>

Ataluren, a 1,2,4-oxadiazole compound, has demonstrated to promote ribosomal readthrough of premature stop codons by rescuing full-length LRBA expression and to improve clinical parameters in a patient harboring a homozygous stop mutation (c. 5047) (C>T) in the LRBA gene.<sup>13</sup>

The recent withdrawal of ataluren's conditional marketing authorization by the EMA, while ensuring continued supply for patients already receiving the drug, underscores the urgent need for alternative therapeutic strategies, such as novel TRIDs.

Three oxadiazole derivatives, NV848, NV914, and NV930, have been validated as translational readthrough promoters in several *in vitro* assays and *in vivo* studies in a wild-type and in nonsense cystic fibrosis CFTR<sup>G542X</sup> mouse model.<sup>14–19</sup> These compounds (patent WO2019101709) were designed to enhance stop codon suppression efficiency and have demonstrated great potential for readthrough across different nonsense-driven disorders.<sup>14,16</sup>

In this study, we conducted a comprehensive evaluation of the readthrough potential of these oxadiazole derivatives in a case of LRBA deficiency due to a homozygous R1683X nonsense mutation. Fibroblasts derived from the patient were used as a model system due to their accessibility through minimally invasive skin biopsy, offering a practical and ethically feasible approach to study treatment response. Herein, we present a detailed analysis of how these compounds affect LRBA transcript stability, restore full-length protein expression and proper cytoplasmic distribution, and reshape the global proteome. Our aim is to confirm the specificity of NV TRIDs in correcting premature stop codons and demonstrate their broad therapeutic potential across various genetic disorders.

## RESULTS

### NV848 treatment increases the mRNA transcript in fibroblast LRBA<sup>R1683X/R1683X</sup>

To evaluate potential cytotoxicity, primary fibroblasts homozygous for the R1683X LRBA mutation were treated chronically with

NV848, NV914, or NV930 at 12  $\mu$ M, along with two positive controls, ataluren at 12  $\mu$ M and G418 (geneticin) at 430  $\mu$ M (Figure 1A), and vehicle as a negative control.

Cells treated with NV848 or NV930 showed a proliferation rate comparable to the vehicle control, indicating no detectable cytotoxic effects. Cells exposed to NV914 showed a slight reduction in proliferation at 48 and 72 h, mirroring the effects observed with ataluren treatment. In contrast, cells treated with G418 exhibited a pronounced and sustained decline in proliferation across all time points, ultimately culminating in extensive cell death (Figure 1B).

Given that PTCs trigger the NMD pathway and reduce transcript abundance, LRBA mRNA levels were measured after treatment with the NV compounds; the observed increase in LRBA mRNA could result from increased transcript stability. Due to the high sensitivity of the cells to G418, this compound was excluded from subsequent experiments. Total RNA was extracted from fibroblasts after 72 h of chronic treatment and subjected to reverse transcription followed by quantitative reverse-transcription PCR (RT-qPCR). LRBA control cells showed a minimum amount of transcript, while cells treated with NV848 showed a significant increase in LRBA mRNA levels compared to those treated with the vehicle control. This increase was not observed in cells exposed to NV914, NV930, or ataluren, suggesting that the condition involving NV848 may contribute to transcript stabilization and facilitate translational readthrough (Figure 1C).

### Chronic treatment with NV848, NV914, and NV930 restores LRBA protein expression in human primary LRBA<sup>R1683X/R1683X</sup> fibroblasts

Restoration of LRBA protein expression and its correct intracellular localization following translational readthrough was assessed by western blot and immunofluorescence analyses. Following 72 h of chronic exposure to NV848, NV914, or NV930, western blot analysis demonstrated the expression of full-length LRBA protein in fibroblasts homozygous for the R1683X mutation. Cells treated with ataluren served as a positive control. In all cases, cells treated with the NV compounds exhibited higher levels of restored protein than those treated with ataluren (Figure 2A).

IMR90 and HeLa cells were also included in the blot to serve as a reference of the protein expression. Notably, HeLa cells showed LRBA expression levels significantly higher than those in IMR90 cells, consistent with a generally higher protein synthesis rate typically observed in cancer cell lines (Figures 2A and 2B). Measurement of band intensities showed a consistent, though not statistically significant, increase in LRBA in fibroblasts treated with TRIDs compared with cells treated only with vehicle. Immunofluorescence analysis confirmed the cytoplasmic localization of the restored LRBA protein in all treated conditions (Figures 2C and 2D). These findings indicate that NV848, NV914, and NV930

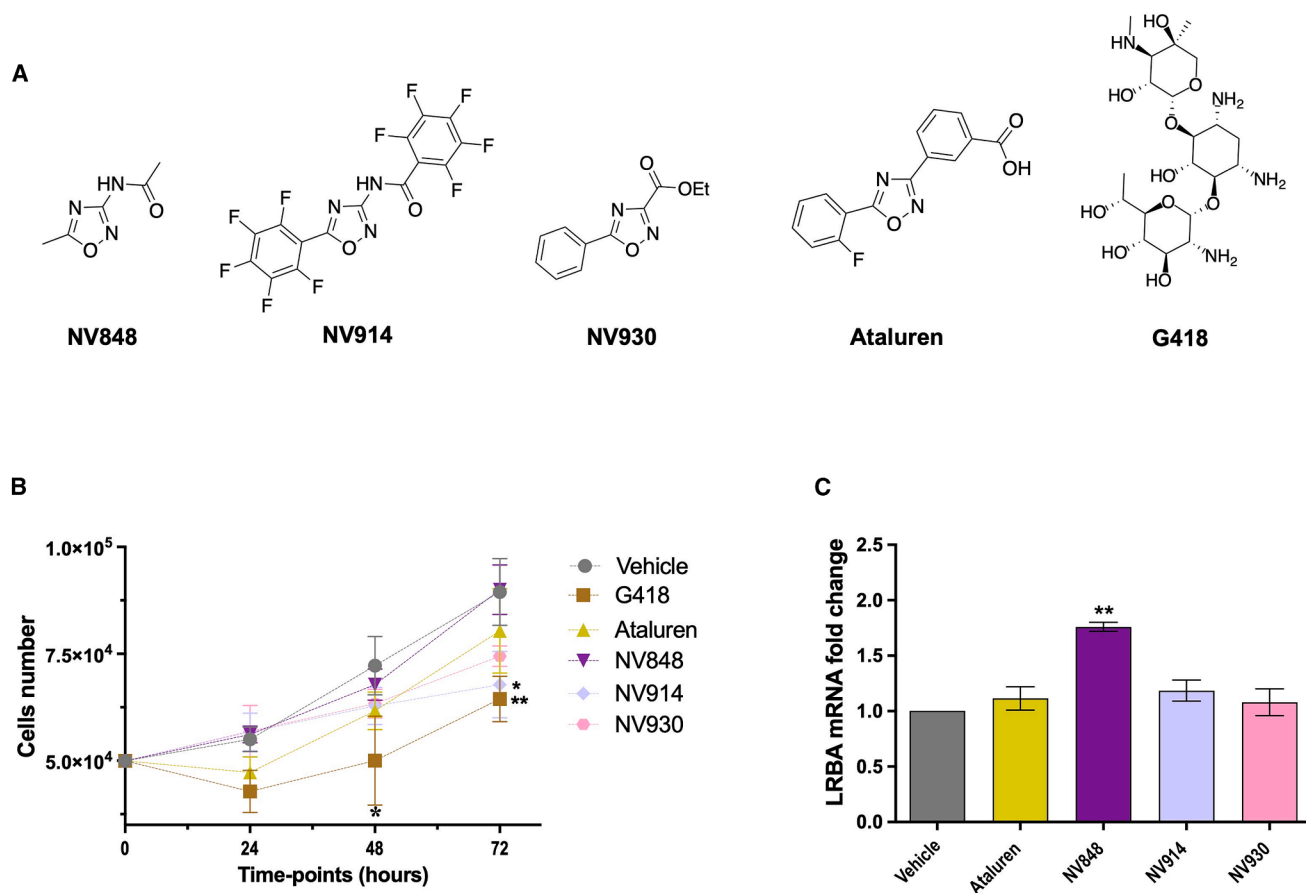


**Figure 1. Compounds and toxicity data**

(A) Chemical structures of readthrough compounds NV848, NV914, NV930, ataluren and G418. (B) Cell growth assay showing fibroblast proliferation per condition (untreated, G418 430  $\mu$ M, ataluren, and NV848, NV914, and NV930 at 12  $\mu$ M). Analyses have been performed in triplicate, and the two-way ANOVA test calculates a  $p$  value summary  $<0.0001$ . (C) LRBA gene expression analyses by real-time PCR were performed for the evaluation of NV TRIDs or ataluren activity (12  $\mu$ M) on LRBA mRNA extracted from primary fibroblasts LRBA<sup>R1683X/R1683X</sup>. The analyses have been conducted in triplicate, showing a  $p$  value  $<0.0001$  calculated by one-way ANOVA.

effectively promote readthrough of the R1683X nonsense mutation, restoring LRBA expression and correct cytoplasmic localization in fibroblasts.

#### Proteomic analysis shows the impact of readthrough compounds

To investigate the global impact of readthrough-inducing compounds on LRBA-deficient fibroblasts, we applied a bottom-up proteomics workflow using label-free liquid chromatography-mass spectrometry. Briefly, cells were lysed, proteins were digested into peptides with trypsin, desalted, and samples were analyzed by high-resolution mass spectrometry to quantify relative protein abundances across all conditions in a data-dependent analysis mode.

Human primary LRBA<sup>R1683X/R1683X</sup> cells were treated chronically for 72 h with ataluren, NV848, NV914, and NV930 at 12  $\mu$ M, or vehicle control, with six independent biological replicates per condition.

Across homozygous fibroblast samples, a total of 4,450 proteins were identified.

Across all fibroblast samples, regardless of treatment, high levels of Vimentin (VIM), an intermediate filament protein typically expressed in these cells, were detected. In addition, proteins commonly abundant in fibroblasts, such as protein S100-A10 and annexin A2 (ANXA2), were also highly expressed.

The analysis revealed high precision, with  $r^2$  values of 0.77, 0.79, 0.81, and 0.85 across biological replicates of the proteome of cells treated with ataluren, NV848, NV914, and NV930, respectively (Figure S1).

Treatment with ataluren and NV848 did not result in statistically significant variation in protein expression. In contrast, NV914 and NV930 induced statistically changes in 11 (Table S1) and 828 proteins (Table S2), respectively (Figure 3A).

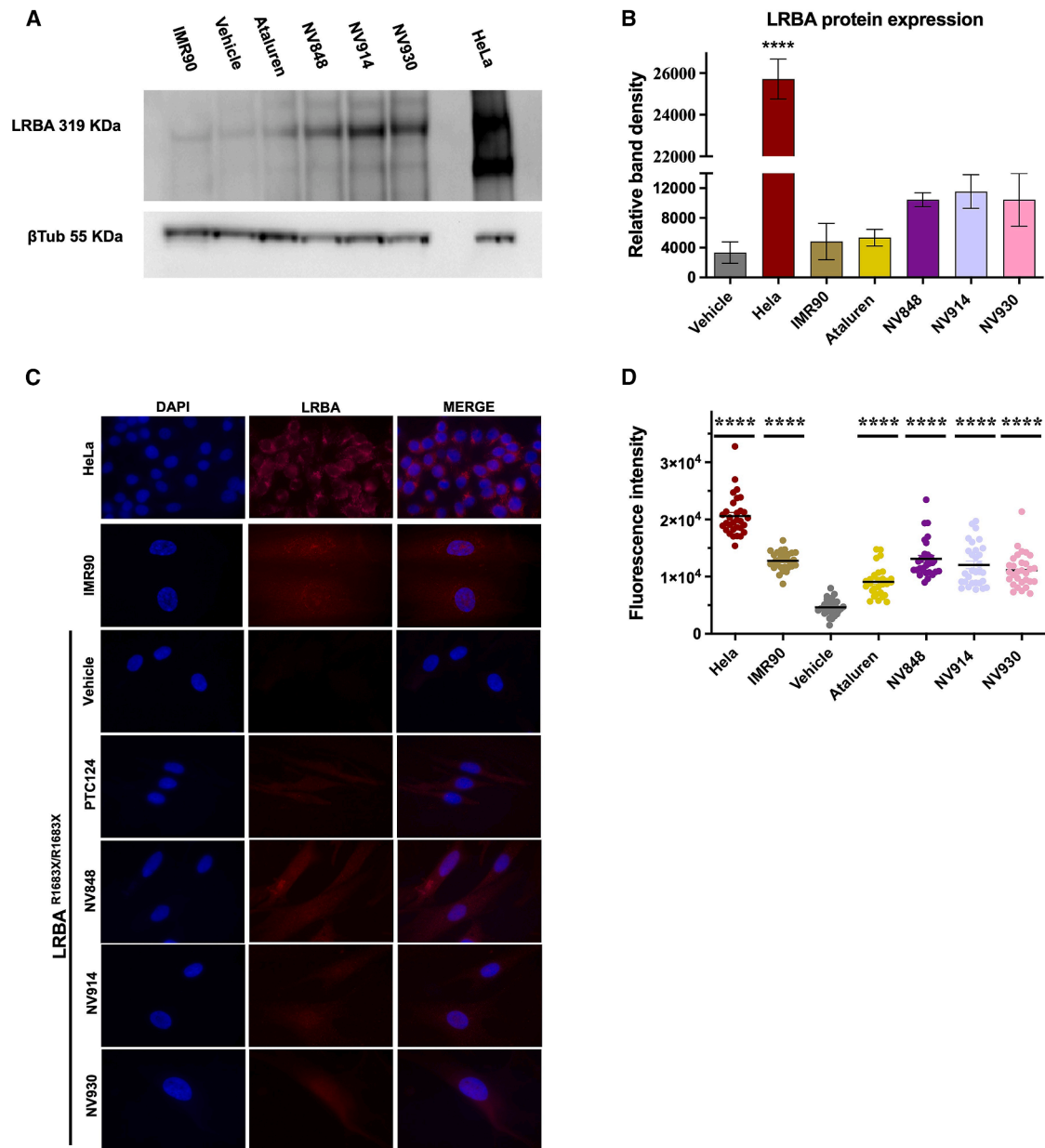


**Figure 2. LRBA rescue after readthrough**

(A) Western blot analysis showing the rescue of LRBA protein (319 KDa) after NV molecules and ataluren treatment.  $\beta$ -tubulin has been used as a loading control. The experiment was performed in triplicate. (B) Western blot bands quantification by ImageJ software, and a  $p$  value  $<0.0001$  was calculated by one-way ANOVA test. (C) Panel showing immunofluorescence analysis results, highlighting the rescue and the correct localization in the cytoplasm of the LRBA protein after 72 h of chronic treatment in fibroblast LRBA<sup>R1683X/R1683X</sup> with NV848, NV914, and NV930 at 12  $\mu$ M. The panel displays DAPI staining for nuclei, LRBA-positive signals, and merged staining. Magnification: 63 $\times$ . (D) Quantification of LRBA fluorescence intensity, analyzed by ImageJ software. The experiment was performed in duplicate, and a one-way ANOVA test statistical analysis showed a  $p$  value  $<0.0001$ .

Particularly, NV914 and NV930 shared six upregulated proteins, including the insulin receptor (INSR), centrin-2 (CETN2), and the spliceosomal factor beta-catenin-like 1 (CTNNBL1) (Figure 3B). Although INSR abundance increased following ataluren and

NV848 treatments, this change did not reach statistical significance after multiple testing correction. The 11 upregulated proteins specific to NV914 showed no detectable connectivity in subsequent network analysis.

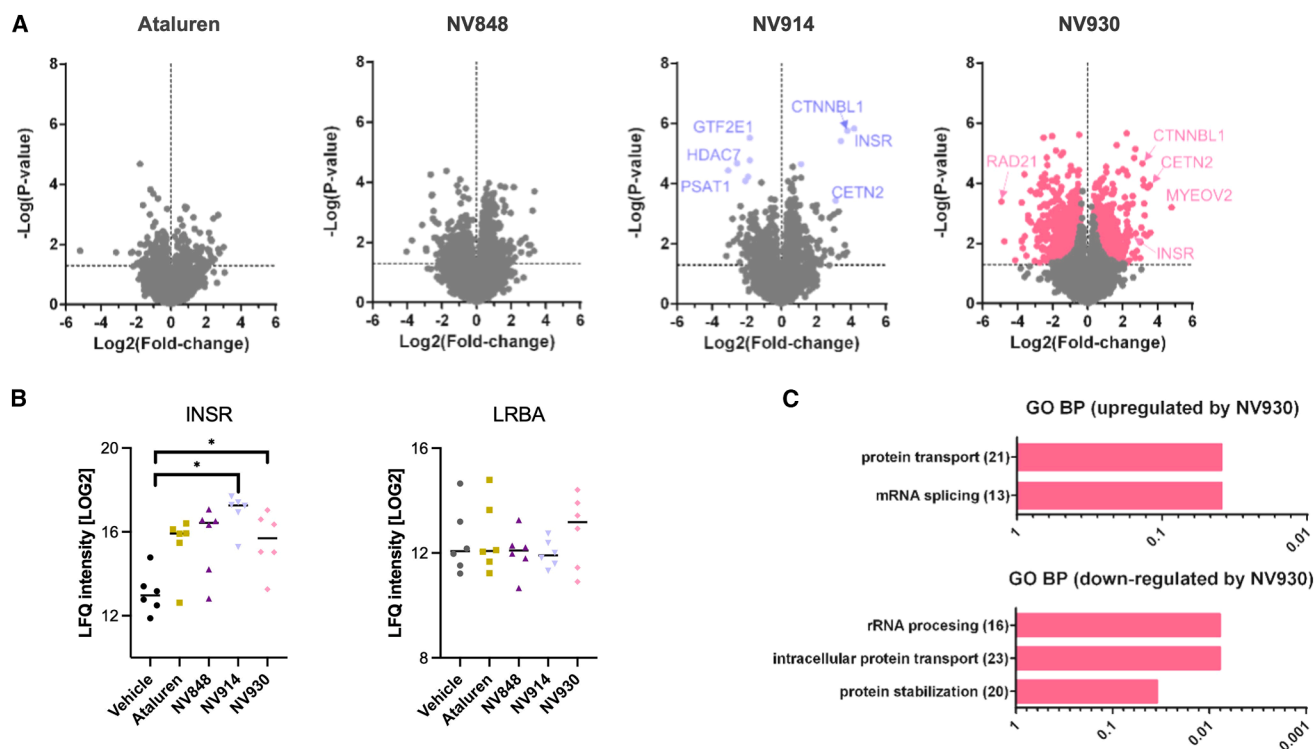


**Figure 3. Proteomic analysis on patient's cells**

(A) Volcano plots of the homozygous cells displaying the proteomic impact of the treatment with ataluren, NV848, NV914, and NV930 from whole-cell lysates (WCLs). Colored proteins exhibit multiple-testing corrected statistical significance. (B) Comparison of Lfq intensities of insulin receptor (INSR) and lipopolysaccharide-responsive and beige-like anchor protein (LRBA) in untreated homozygous cells and upon treatment. \*adj.  $p$  value  $< 0.05$ . (C) Gene Ontology term enrichments of biological processes (GO BP) of the NV930-treated homozygous cells. The reported terms show an adjusted  $p$  value  $< 0.05$ .

Gene Ontology enrichment analysis for biological processes was performed on the 303 proteins upregulated by NV930 treatment (Figure 3C). Interestingly, only two terms were significantly enriched, corresponding to protein transport (21 proteins, Benjamini-Hochberg adjusted  $p$  value = 0.039) and mRNA splicing (13 proteins, Benjamini-Hochberg adjusted  $p$  value = 0.039). The target protein, LRBA, was not connected with any of the upregulated proteins in the network analysis. Similarly, analysis of the 525 down-regulated proteins revealed modest enrichment for biological processes, including rRNA processing (16 proteins, Benjamini-Hochberg adjusted  $p$  value = 0.035), intracellular protein transport (23 proteins, Benjamini-Hochberg adjusted  $p$  value = 0.0078), and protein stabilization (20 proteins, Benjamini-Hochberg adjusted  $p$  value = 0.0078). However, despite their term enrichment statistics, the proteins in these groups did not exhibit strong connectivity in network analysis.

LRBA was detected in all samples; however, label-free quantification showed that it was not possible to detect statistically significant changes in LRBA levels by treatment with readthrough-inducing compounds, relative to the vehicle control, which may be due to analyzing proteomes from whole-cell lysates.

Overall, homozygous LRBA-deficient fibroblasts exhibit a rigid proteomic response to TRID treatment, with minimal global remodeling except in the case of NV930, where evidence shows the involvement of vesicular transport and RNA splicing pathways.

## DISCUSSION

In this work, we evaluated the readthrough efficacy and downstream proteomic effects of three oxadiazole derivatives, NV848, NV914, and NV930, compared to ataluren, in fibroblasts derived from a patient homozygous for the LRBA R1683X nonsense mutation. All compounds successfully restored full-length LRBA protein expression, as shown by western blot analysis, and correctly relocalized the protein to the cytoplasm, as shown by immunofluorescence.

Western blot analysis confirmed that all NV compounds outperformed ataluren in promoting readthrough of the premature stop codon, with NV848 showing the highest readthrough efficiency.

It also fully preserved cell proliferation and uniquely increased LRBA mRNA levels, suggesting an additional stabilizing effect on the transcript.

Both NV914 and NV930 induced readthrough but did not stabilize LRBA mRNA. Moreover, NV914 caused a moderate reduction in cell proliferation, similar to ataluren, whereas NV930 had no significant effect compared to untreated controls.

Shotgun proteomic analysis revealed important differences among the compounds. NV848 did not cause significant variation in the global proteome, indicating a high degree of specificity and minimal off-target engagement. NV914 modulated the expression of only 11 proteins, none of which were connected in network analysis. In contrast, NV930 modulated 828 proteins, with enrichment in pathways such as vesicular transport and mRNA splicing. It seems that the magnitude of the proteome perturbation indicates the high specificity of the TRIDs, with NV930 being the least specific among the three molecules.

While methods such as western blot and mRNA quantification confirm the recovery of the protein of interest, proteomic profiling enables the detection of broader impact that would otherwise remain undetectable, thus emphasizing the value of global proteomic analysis as a complementary tool in drug evaluation.

While our results clearly demonstrate efficient readthrough and restoration of LRBA expression in fibroblasts carrying the homozygous mutation LRBA<sup>R1683X/R1683X</sup>, it should be noted that readthrough efficiency may vary depending on the specific stop codon and its surrounding nucleotide context, as well as on mRNA levels influenced by activation of the nonsense-mediated decay (NMD) pathway. These factors could affect the extent of LRBA rescue observed and underscore the importance of assessing NV compound activity across additional LRBA nonsense variants.

Considering the positive outcome of the single clinical trial with ataluren in the patient carrying the homozygous R1683X mutation in the LRBA gene (LRBA<sup>R1683X/R1683X</sup>),<sup>13</sup> the positive rescue of LRBA observed by western blot and immunofluorescence analysis in this study, higher than that observed by ataluren treatment, opens good perspectives for our NV lead compounds for further preclinical development.

In conclusion, our data establish NV molecules as leading candidates for correcting LRBA nonsense mutations, suggesting NV848 as the most promising candidate, displaying superior activity, minimal off-target proteomic effects, and a unique ability to stabilize LRBA mRNA.

These results lay the foundation for further investigation of their potential in treating other genetic disorders caused by premature stop codons, thereby expanding therapeutic options for monogenic diseases.

## MATERIALS AND METHODS

### Chemistry

All solvents and reagents were obtained from commercial sources. Ataluren and NV molecules have been synthesized as reported in

the literature.<sup>14,20</sup> G418 sulfate (geneticin) was purchased from Thermo Fisher Scientific.

NV848: <sup>1</sup>H NMR (DMSO-d<sub>6</sub>) δ (ppm): 2.08 (s, 3H), 2.52 (s, 3H), 10.94 (s, 1H). High-resolution mass spectrometry (HRMS) for C<sub>5</sub>H<sub>7</sub>N<sub>3</sub>O<sub>2</sub> found 142.0625 [M + H]<sup>+</sup> (Calcd. 142.0611).

NV914: HRMS for C<sub>15</sub>HF<sub>10</sub>N<sub>3</sub>O<sub>2</sub> found 445.9989 [M + H]<sup>+</sup> (Calcd. 445.9982).

NV930: <sup>1</sup>H NMR (DMSO-d<sub>6</sub>) δ (ppm): 8.16 (d, 2H), 7.80–7.71 (m, 1H), 7.66 (t, 2H), 4.45 (q, 2H), 1.36 (t, 3H). HRMS for C<sub>11</sub>H<sub>10</sub>N<sub>2</sub>O<sub>3</sub> found 219.0772 [M + H]<sup>+</sup> (Calcd. 219.0764).

Ataluren: <sup>1</sup>H NMR (DMSO-d<sub>6</sub>) δ (ppm): 13.37 (s, 1H), 8.63 (td, 1H), 8.39–8.31 (m, 1H), 8.18 (dt, 2H), 7.87–7.71 (m, 2H), 7.62–7.45 (m, 2H). HRMS for C<sub>15</sub>H<sub>9</sub>FN<sub>2</sub>O<sub>3</sub> found 285.0682 [M + H]<sup>+</sup> (Calcd. 285.067).

### Cell culture

All human samples were collected and analyzed according to the standards of the ethical committee and the Declaration of Helsinki, following obtaining written consent. The patient gave written informed consent for skin biopsy, fibroblast culture.

Fibroblasts derived from the patient carrying the homozygous R1683X mutation in the LRBA gene (LRBA<sup>R1683X/R1683X</sup>) were cultured in T25 flasks at 37°C with 5% CO<sub>2</sub>. Cells were maintained in Minimum Essential Medium Eagle (MEM 1×; Gibco, Thermo Fisher Scientific, USA) supplemented with 2% Ultrosor G (Fisher Scientific, Thermo Fisher Scientific, USA), 1% L-glutamine (Invitrogen, Thermo Fisher Scientific, USA), and 1% non-essential amino acids (Gibco, Thermo Fisher Scientific, USA).

### Cell proliferation assay

Fibroblast LRBA<sup>R1683X/R1683X</sup> proliferation was assessed under chronic treatment conditions. Cells were seeded at 50,000 cells per well in 12-well plates (Corning, USA) in duplicate. At time 0, cells received fresh culture medium containing one of the following: NV848, NV914, NV930, or ataluren at 12 μM (from 100 mM DMSO stock diluted to 1 mM in DPBS 1×), or G418 at 430 μM; vehicle served as a negative control. After 24 h and again at 48 h, the medium was completely replaced with freshly prepared medium containing the same compound at the same concentration. Cell counts were performed at 24, 48, and 72 h using a Bürker chamber. Each condition was measured in triplicate.

### RNA extraction

For RNA extraction, 300,000 LRBA<sup>R1683X/R1683X</sup> fibroblasts were seeded in T25 flasks and treated chronically with NV848, NV914, NV930, or ataluren. The culture medium was replaced daily with fresh medium containing the respective compound at the chosen concentration to ensure continuous exposure. At the end of

treatment period, cells were detached with 0.05% trypsin (Thermo Fisher Scientific, USA), collected, pelleted, and lysed with RLT buffer containing  $\beta$ -mercaptoethanol. RNA was extracted using the RNeasy Mini Kit (QIAGEN, Germany) following the manufacturer's protocol, including on-column DNase treatment. RNA integrity was assessed via 1% agarose gel electrophoresis, and concentrations were measured using a NanoDrop 2000 spectrophotometer (Thermo Scientific, Invitrogen, USA).

#### Quantitative PCR

Complementary DNA (cDNA) was synthesized from 1  $\mu$ g of total RNA using the High-Capacity cDNA Reverse Transcription Kit (Thermo Fisher Scientific, USA). Quantitative PCR was performed using SYBR Green Master Mix (Life Technologies, Thermo Fisher Scientific, USA) with specific primers for LRBA (forward: 5'-TCCGAGCCCTCAATGTGTTC-3'; reverse: 5'-CATGGCAGAACCTCTGGGAG-3') and GAPDH as the housekeeping gene (forward: 5'-CTCATGACCACAGTCCATGCC-3'; reverse: 5'-GCCATCCACAGTCTTCTGGGT-3'). Reactions were run in triplicate on a 7300 Real-Time PCR System (Applied Biosystems) and analyzed using the 7300 System Software.

#### Protein extraction

For protein extraction, 250,000 fibroblasts per condition were seeded in T25 flasks and exposed to the same chronic treatment regimen as described earlier. Following 72 h, cells were lysed in RIPA buffer (Pierce RIPA Buffer, Thermo Scientific) supplemented with 1% protease inhibitor cocktail (Halt Protease and Phosphatase Inhibitor Cocktail, Thermo Scientific) on ice for 90 min. Lysates were centrifuged at 12,000 rpm for 20 min at 4°C, and supernatants were collected. Protein concentrations were determined using the Bradford assay.

#### Western blotting

For western blot analysis, 30  $\mu$ g of protein per sample was separated on 3%–8% SDS-PAGE NuPAGE gels (Invitrogen, Thermo Fisher Scientific, USA) run at 150 V and 100 mA for 1 h. Proteins were then transferred onto PVDF membranes (Invitrogen, Thermo Fisher Scientific, USA) overnight at 4°C at 12 V and 50 mA. Membranes were blocked with 5% non-fat milk in TBS-T (Pierce TBS-Tween 20 $\times$ , Invitrogen, Thermo Fisher Scientific, USA) for 1 h at room temperature and incubated overnight at 4°C with primary antibodies: anti-LRBA (1:1,000; Bethyl Laboratories Inc., USA) and anti- $\beta$ -tubulin (1:5,000; Sigma-Aldrich, USA). Membranes were washed three times with TBS-TWEEN 1X for 15 min and then incubated with horseradish peroxidase (HRP)-conjugated secondary antibodies, anti-rabbit (Promega, USA) 1:3,000, and anti-mouse (Invitrogen, Thermo Fisher Scientific, USA) 1:5,000, respectively. Following three additional washes, detection was performed using SuperSignal West Femto Maximum Sensitivity Substrate (Thermo Scientific) and visualized with a Chemidoc XRS system (Bio-Rad). Band intensities were quantified using ImageJ software (NIH).

#### Immunofluorescence

To assess LRBA protein localization, 50,000 LRBA<sup>R1683X/R1683X</sup> fibroblasts were seeded on coverslips in 12-well plates and subjected to chronic treatment for 72 h. Cells were fixed with ice-cold methanol and washed three times with PBS 1 $\times$ . Permeabilization was performed with 0.01% Triton X-100 for 10 min, followed by two washes in PBS 1 $\times$ . Blocking was carried out with 0.1% BSA for 1 h at room temperature. Cells were incubated overnight at 4°C with anti-LRBA primary antibody (1:100; Bethyl Laboratories Inc., USA), and, after three washes in PBS, cells were incubated with Alexa Fluor 647-conjugated anti-rabbit secondary antibody (1:500; Thermo Fisher Scientific, USA) for 1 h at room temperature. Nuclei were stained with DAPI, and coverslips were mounted for imaging. Fluorescence images were captured using an AxioVision microscope (Zeiss) at 63 $\times$  magnification and analyzed with ImageJ software (NIH). Experiments were performed in duplicate.

#### Proteomic analysis

##### Sample preparation

Primary fibroblast cultures from the LRBA-deficient patient were subjected under five conditions (vehicle control, ataluren, NV848, NV914, and NV930). For each treatment, 250,000 cells were seeded in 60 mm dishes and allowed to adhere for 24 h. The culture medium was then replaced daily with fresh medium containing the respective compound at 12  $\mu$ M, ensuring continuous exposure over the 72-h treatment period. At the end of treatment, cell morphology was recorded by phase-contrast microscopy before samples were placed on ice. Plates were washed twice with 1 mL PBS, aspirated thoroughly, and lysed with 130  $\mu$ L of sodium dodecyl sulfate (SDS) lysis buffer. Lysates were heated at 95°C for 5 min with shaking at 1,400 rpm and then stored at –20°C until digestion.

##### Protein digestion

Whole-cell lysates (WCLs) were proteolytically digested using a modified EasyPhos protocol.<sup>21</sup> WCLs were thawed and reheated at 95°C for 5 min at 1,400 rpm. After cooling to room temperature, protein concentrations were measured by bicinchoninic acid assay. An amount of 20  $\mu$ g of total protein per sample was reduced and alkylated using tris(2-carboxyethyl)phosphine and 2-chloroacetamide at 45°C for 5 min. Proteins were subsequently digested with Trypsin/Lys-C at a 1:100 enzyme-to-substrate ratio for 18 h at 37°C. Following digestion, the samples were reconstituted in styrenedivinylbenzene-reverse phase sulfonate (SDB-RPS) loading buffer consisting of 99% isopropanol and 1% trifluoroacetic acid (TFA) and then desalted using SDB-RPS StageTips.

Samples were reconstituted in 5  $\mu$ L of 30% formic acid containing 10 fmol of synthetic standard peptides and subsequently diluted with 40  $\mu$ L of loading solvent composed of 98% water, 2% acetonitrile, and 0.05% TFA. Peptides were reconstituted in 15  $\mu$ L of MS loading buffer containing 97.7% water, 2% acetonitrile, and 0.3% TFA.

### LC-MS/MS analysis

Liquid chromatography-tandem mass spectrometry (LC-MS/MS) analysis was carried out using a timsTOF Pro mass spectrometer (Bruker Daltonics, Bremen, Germany) coupled to a Dionex UltiMate 3000 RSLCnano system (Thermo Scientific, Bremen, Germany). WCL samples were analyzed by label-free quantification (LFQ) shotgun proteomics, following a method previously described in the literature.<sup>22</sup> An injection volume of 2  $\mu$ L was used for each sample. Peptides were initially loaded onto an Acclaim PepMap C18 pre-column (2 cm  $\times$  100  $\mu$ m, 100  $\text{\AA}$ ; Thermo Fisher Scientific, Vienna, Austria) at a flow rate of 10  $\mu$ L per minute using loading buffer. After trapping, peptides were eluted at a flow rate of 300 nL per minute and separated on an Aurora series CSI UHPLC emitter column (25 cm  $\times$  75  $\mu$ m, 1.6  $\mu$ m C18; Ionopticks, Fitzroy, Australia). A linear gradient of 8%–40% mobile phase B, consisting of 79.9% acetonitrile, 20% water, and 0.1% formic acid, in mobile phase A, consisting of 99.9% water and 0.1% formic acid, was applied over 95 min.

The captive ion spray source was run at 1.6 kV. Data were acquired in PASEF mode using 10 PASEF cycles per acquisition with a total cycle time of 1.16 s and a target intensity threshold of 2,500.

### Data processing

MaxQuant (version 1.6.17.0), including the Andromeda search engine, was used for label-free quantification of the proteomic raw data. Non-redundant SwissProt entries were searched, requiring at least two peptides for identification, one of which had to be unique. The peptide tolerance for the first search was set to 40 ppm, while the main search peptide tolerance was 20 ppm. The false discovery rate (FDR) was fixed at 0.01 at both the peptide and protein levels, with a maximum of two missed cleavages allowed. The match between runs option was enabled.

The search criteria included carbamidomethylation of cysteine as a fixed modification and oxidation of methionine, along with N-terminal acetylation as dynamic modifications. The fibroblast samples were searched together with the cytoplasmic fraction of an untreated A2780 ovarian cancer cell line to enhance confidence in identifying LRBA. The A2780 samples were not included in the statistical evaluation, which was carried out using Perseus software (version 1.6.14) and LFQ intensities derived from the MaxQuant result files.

Statistical significance was determined by permutation-based FDR (set to 0.05) and  $S_0 = 0.1$  for  $t$  tests, which provided multiple-testing corrected significant protein regulations due to perturbations.

### DATA AND CODE AVAILABILITY

Data are available directly from the corresponding authors upon request.

### ACKNOWLEDGMENTS

The research leading to these results has received funding from the European Union - NextGenerationEU through the Italian Ministry of University and Research under PNRR-M4C2-I1.3 Project PE\_00000019 "HEAL ITALIA" to I.P. and L.L. (University of Palermo), CUP B73C22001250006 and PRJ-0863 PRIN2022 to I.P. (University of Pa-

lermo), and CUP B53D23008390006. The views and opinions expressed are those of the authors only and do not necessarily reflect those of the European Union or the European Commission. Neither the European Union nor the European Commission can be held responsible for them.

### AUTHOR CONTRIBUTIONS

Conceptualization, I.P. and L.L.; methodology, L.L., I.P., and S.M.-M.; investigation, I.F., E.V., R.V., D.R., S.M., A.Z., A.C., Y.B., A.B., and S.M.-M.; visualization, A.P., M.M., and S.M.-M.; funding acquisition, I.P. and L.L.; project administration, I.P. and L.L.; supervision, I.P. and L.L.; writing – original draft, I.F., E.V., L.L., S.M.-M., and I.P.; writing – review and editing, I.F., E.V., R.V., D.R., S.M., A.Z., A.P., A.C., M.M., Y.B., A.B., S.M.-M., L.L., and I.P. All authors have read, edited, and approved the final manuscript.

### DECLARATION OF INTERESTS

I.P., L.L., and A.P. are co-inventors on patents related to the oxadiazole-based TRIDs described in this study. These compounds have been licensed to CCM Bioscience Inc.; I.P. is a scientific advisor to CCM Bioscience Inc.

### SUPPLEMENTAL INFORMATION

Supplemental information can be found online at <https://doi.org/10.1016/j.omtn.2025.102808>.

### REFERENCES

- Poli, M.C., Aksentijevich, I., Bousfiha, A.A., Cunningham-Rundles, C., Hambleton, S., Klein, C., Morio, T., Picard, C., Puel, A., Rezaei, N., et al. (2025). Human inborn errors of immunity: 2024 update on the classification from the International Union of Immunological Societies Expert Committee. *J. Hum. Immun. 1*, e20250003. <https://doi.org/10.70962/jhi.20250003>.
- Romanov, G.A., and Sukhoverov, V.S. (2017). Arginine CGA codons as a source of nonsense mutations: a possible role in multivariant gene expression, control of mRNA quality, and aging. *Mol. Genet. Genomics 292*, 1013–1026. <https://doi.org/10.1007/s00438-017-1328-y>.
- Vitale, E., Ricci, D., Corrao, F., Fiduccia, I., Cruciat, I., Carollo, P.S., Branchini, A., Lentini, L., and Pibiri, I. (2025). Nonsense Mutations in Rare and Ultra-Rare Human Disorders: An Overview. *IUBMB Life 77*, e70031. <https://doi.org/10.1002/iub.70031>.
- Palma, M., and Lejeune, F. (2021). Deciphering the molecular mechanism of stop codon readthrough. *Biol. Rev. Camb. Philos. Soc. 96*, 310–329. <https://doi.org/10.1111/brv.12657>.
- Monaghan, L., Longman, D., and Cáceres, J.F. (2023). Translation-coupled mRNA quality control mechanisms. *EMBO J. 42*, e114378. <https://doi.org/10.15252/embj.2023114378>.
- Martinez Jaramillo, C., and Trujillo-Vargas, C.M. (2018). LRBA in the endomembrane system. *Colomb. Méd. 49*, 236–243. <https://doi.org/10.25100/cm.v49i2.3802>.
- Lopez-Herrera, G., Tampella, G., Pan-Hammarström, Q., Herholz, P., Trujillo-Vargas, C.M., Phadwal, K., Simon, A.K., Moutschen, M., Etzioni, A., Mory, A., et al. (2012). Deleterious mutations in LRBA are associated with a syndrome of immune deficiency and autoimmunity. *Am. J. Hum. Genet. 90*, 986–1001. <https://doi.org/10.1016/j.ajhg.2012.04.015>.
- Alkhairy, O.K., Abolhassani, H., Rezaei, N., Fang, M., Andersen, K.K., Chavoshzadeh, Z., Mohammadzadeh, I., El-Rajab, M.A., Massaad, M., Chou, J., et al. (2016). Spectrum of Phenotypes Associated with Mutations in LRBA. *J. Clin. Immunol. 36*, 33–45. <https://doi.org/10.1007/s10875-015-0224-7>.
- Gámez-Díaz, L., August, D., Stepensky, P., Revel-Vilk, S., Seidel, M.G., Noriko, M., Morio, T., Worth, A.J.J., Blessing, J., Van de Veerdonk, F., et al. (2016). The extended phenotype of LPS-responsive beige-like anchor protein (LRBA) deficiency. *J. Allergy Clin. Immunol. 137*, 223–230. <https://doi.org/10.1016/j.jaci.2015.09.025>.
- Delmonte, O.M., Castagnoli, R., Calzoni, E., and Notarangelo, L.D. (2019). Inborn Errors of Immunity With Immune Dysregulation: From Bench to Bedside. *Front. Pediatr. 7*, 353. <https://doi.org/10.3389/fped.2019.00353>.
- Campofelice, A., Lentini, L., Di Leonardo, A., Melfi, R., Tutone, M., Pace, A., and Pibiri, I. (2019). Strategies against Nonsense: Oxadiazoles as Translational Readthrough-Inducing Drugs (TRIDs). *Int. J. Mol. Sci. 20*, 3329. <https://doi.org/10.3390/ijms20133329>.

12. Ricci, D., Cruciata, I., Fiduccia, I., Vitale, E., Corrao, F., Branchini, A., Carollo, P.S., Pibiri, I., and Lentini, L. (2025). Advancing Therapeutic Strategies for Nonsense-Related Diseases: From Small Molecules to Nucleic Acid-Based Innovations. *IUBMB Life* 77, e70027. <https://doi.org/10.1002/iub.70027>.
13. Lentini, L., Perriera, R., Corrao, F., Melfi, R., Tutone, M., Carollo, P.S., Fiduccia, I., Pace, A., Ricci, D., Genovese, F., et al. (2025). A Precision Medicine Approach to Primary Immunodeficiency Disease: Ataluren Strikes Nonsense Mutations Once Again. *Mol. Ther.* 33, 3231–3241. <https://doi.org/10.1016/j.ymthe.2025.03.045>.
14. Pibiri, I., Melfi, R., Tutone, M., Di Leonardo, A., Pace, A., and Lentini, L. (2020). Targeting Nonsense: Optimization of 1,2,4-Oxadiazole TRIDs to Rescue CFTR Expression and Functionality in Cystic Fibrosis Cell Model Systems. *Int. J. Mol. Sci.* 21, 6420. <https://doi.org/10.3390/ijms21176420>.
15. Corrao, F., Zizzo, M.G., Tutone, M., Melfi, R., Fiduccia, I., Carollo, P.S., Leonardo, A.D., Caldara, G., Perriera, R., Pace, A., et al. (2022). Nonsense codons suppression. An acute toxicity study of three optimized TRIDs in murine model, safety and tolerability evaluation. *Biomed. Pharmacother.* 156, 113886. <https://doi.org/10.1016/j.biopha.2022.113886>.
16. Bezzetti, V., Lentini, L., Api, M., Busilacchi, E.M., Cavalieri, V., Pomilio, A., Diomede, F., Pegoraro, A., Cesaro, S., Poloni, A., et al. (2022). Novel Translational Read-through-Inducing Drugs as a Therapeutic Option for Shwachman-Diamond Syndrome. *Biomedicines* 10, 886. <https://doi.org/10.3390/biomedicines10040886>.
17. Carollo, P.S., Tutone, M., Culetta, G., Fiduccia, I., Corrao, F., Pibiri, I., Di Leonardo, A., Zizzo, M.G., Melfi, R., Pace, A., et al. (2023). Investigating the Inhibition of FTSJ1, a Tryptophan tRNA-Specific 2'-O-Methyltransferase by NV TRIDs, as a Mechanism of Readthrough in Nonsense Mutated CFTR. *Int. J. Mol. Sci.* 24, 9609. <https://doi.org/10.3390/ijms24119609>.
18. Perriera, R., Vitale, E., Pibiri, I., Carollo, P.S., Ricci, D., Corrao, F., Fiduccia, I., Melfi, R., Zizzo, M.G., Tutone, M., et al. (2023). Readthrough Approach Using NV Translational Readthrough-Inducing Drugs (TRIDs): A Study of the Possible Off-Target Effects on Natural Termination Codons (NTCs) on TP53 and Housekeeping Gene Expression. *Int. J. Mol. Sci.* 24, 15084. <https://doi.org/10.3390/ijms242015084>.
19. Fiduccia, I., Corrao, F., Zizzo, M.G., Perriera, R., Genovese, F., Vitale, E., Ricci, D., Melfi, R., Tutone, M., Pace, A., et al. (2024). Promoting readthrough of nonsense mutations in CF mouse model: Biodistribution and efficacy of NV848 in rescuing CFTR protein expression. *Mol. Ther.* 32, 4514–4523. <https://doi.org/10.1016/j.ymthe.2024.10.028>.
20. Lentini, L., Melfi, R., Di Leonardo, A., Spinello, A., Barone, G., Pace, A., Palumbo Piccionello, A., and Pibiri, I. (2014). Toward a rationale for the PTC124 (Ataluren) promoted readthrough of premature stop codons: a computational approach and GFP-reporter cell-based assay. *Mol. Pharm.* 11, 653–664. <https://doi.org/10.1021/mp400230s>.
21. Humphrey, S.J., Karayel, O., James, D.E., and Mann, M. (2018). High-throughput and high-sensitivity phosphoproteomics with the EasyPhos platform. *Nat. Protoc.* 13, 1897–1916. <https://doi.org/10.1038/s41596-018-0014-9>.
22. Bortel, P., Hagn, G., Skos, L., Bileck, A., Paulitschke, V., Paulitschke, P., Gleiter, L., Mohr, T., Gerner, C., and Meier-Menches, S.M. (2024). Memory effects of prior sub-culture may impact the quality of multiomic perturbation profiles. *Proc. Natl. Acad. Sci. USA* 121, e2313851121. <https://doi.org/10.1073/pnas.2313851121>.